Rare Met. (2021) 40(9):2523–2529
https://doi.org/10.1007/s12598-020-01496-0

RARE METALS
www.editorialmanager.com/rmet

Fatigue crack growth behavior of 2624-T39 aluminum alloy with different grain sizes

Guan Huang, Zhi-Hui Li*, Li-Ming Sun, Xi-Wu Li, Kai Wen, Li-Zhen Yan, Bai-Qing Xiong, Yong-An Zhang

Received: 12 July 2019 / Revised: 8 October 2019 / Accepted: 16 June 2020 / Published online: 6 July 2020

Abstract The microstructure of 2624-T39 aluminum alloy was analyzed by means of metallographic (OM), scanning electron microscope (SEM) and transmission electron microscope (TEM). The effects of different microstructure characteristics on the tensile properties and fatigue crack growth rate of 2624-T39 aluminum alloy were studied. Results showed that the grain size of the alloy was a typical fiber structure along the rolling direction, and the main second phase was the Al_2CuMg phase. The grain size of the alloy had an obvious influence on the fatigue crack growth rate, and the alloy showed a lower fatigue crack growth rate due to the larger grain size. The crack initiation zone on the fracture surface of alloys with lower fatigue crack growth rate was relatively rough, the crack propagation zone had obvious fatigue striations, and the transient fracture zone had a large number of smaller dimples.

Keywords 2624-T39 aluminum alloy; Grain size; Fatigue crack growth rate; Fatigue fracture morphology

G. Huang, Z.-H. Li*, X.-W. Li, K. Wen, L.-Z. Yan, B.-Q. Xiong, Y.-A. Zhang
State Key Laboratory of Nonferrous Metals and Processes, GRINM Group Co., Ltd., Beijing 100088, China
e-mail: lzh@grinm.com

G. Huang, X.-W. Li, K. Wen, L.-Z. Yan, Y.-A. Zhang
GRIMAT Engineering Institute Co., Ltd., Beijing 101407, China

G. Huang, Z.-H. Li, X.-W. Li, L.-Z. Yan, B.-Q. Xiong, Y.-A. Zhang
General Research Institute for Nonferrous Metals, Beijing 100088, China

L.-M. Sun
Northeast Light Alloy Co., Ltd., Harbin 150060, China

1 Introduction

2X24 series aluminum alloys have good comprehensive properties such as high strength, high toughness, low density and fatigue resistance [1]. Typical 2X24 series aluminum alloys, such as 2024-T3 and 2124-T3, have been widely used in aviation, aerospace and civil industries [2, 3]. With the rapid development of the aerospace industry in recent years, the damage tolerance performance requirements of 2X24 aluminum alloy have been further improved [4]. The materials need not only high static strength but also superior corrosion resistance, fracture toughness, fatigue crack growth resistance and other properties. 2424 and 2524 aluminum alloys were designed by Alcoa based on 2024 aluminum alloy, to furtherly reduce the impurity content of Si and Fe and adjust the composition range of main alloying elements. Compared with 2024-T3 aluminum alloy in the same strength, 2524-T3 aluminum alloy possesses significantly better fatigue strength and fracture toughness. Although the strength of 2024-T3 and 2524-T3 is almost the same, the fatigue strength and fracture toughness of 2524-T3 are significantly higher than those of 2024-T3. It is an ideal material for fuselage skin, which has been widely used in large aircraft [5, 6]. Then, in 2009, Alcoa registered 2624 aluminum alloy, of which impurity Fe and Si contents are lower than those of 2524 aluminum alloy, and its melt is purer, which is the ideal aluminum alloy to replace 2524, further improving the competitiveness of 2X24 series aluminum alloy in the aircraft industry [7]. However, there are relatively few reports on 2624 aluminum alloys at home and abroad.

The fatigue properties are mainly affected by grain size, undissolved coarse phase, medium-size second phase and fine aging precipitation. The undissolved coarse phase may break or separate from the substrate under cyclic loading,

thus providing a preferential path for fatigue crack growth and accelerating fatigue crack growth [8]. The bridging effect of a medium-size second phase can reduce the crack growth rate [9]. As the content of the second phase increases, the fatigue crack growth rate also increases [10]. However, the effect of grain size on fatigue expansion is still controversial. Firstly, Saga et al. [11] believed that the smaller the grain size is, the lower the fatigue crack growth rate is. Subsequently, Lindigkeit et al. [12] and Carter et al. [13] found that the crack growth rate slowed down with the increase of grain size. In recent years, there have been studies on the effect of grain size on the crack growth rate of 2524 aluminum alloy sheets. Shou et al. [14] found that the effect of grain size on the crack growth rate was caused by the crack closure. Yin et al. [15] found that the fatigue crack growth rate of coarse-grained samples would decrease, and the crack deflection model was used to reveal this phenomenon. In conclusion, the effect of grain size on fatigue crack growth needs to be proved by new experiments.

To furtherly investigate the effect of grain size on the fatigue crack growth rate, various methods were used to obtain alloys with different grain sizes, such as electrodeposition, equal-channel angular pressure, and rolling deformation [16–19]. In order to eliminate the influence of external conditions on the samples, the 2624-T39 aluminum alloy thick plate was adopted to analyze the influence of microstructure characteristics with different thicknesses on the fatigue crack growth rate.

2 Experimental

The experimental material was a 26-mm-thick 2624-T39 aluminum plate and the chemical composition was 4.38 wt% Cu, 1.35 wt% Mg, 0.60 wt% Mn, 0.036 wt% Fe, and 0.014 wt% Si, and the balance was Al. The experimental materials were mainly taken from different thickness (D) positions of the thick plate.

The manufacturing process and heat treatment parameters of thick alloy plate were as follows: homogenization annealing (450 °C/16 h); ultrasonic inspection after milling surface (grade B); hot rolled into thick plate; solid solution (495 °C/1 h); water quenching (< 39 °C); straightening and pre-aging (room temperature/7 h); 11% pre-deformation before natural aging for 96 h.

The tensile test samples were manufactured along longitudinal (L) and transverse (LT) directions at room temperature, and then were tested on AG-501CNE electronic tensile test machine in accordance with GB/T228-2009 metal tensile test at room temperature. The average values of three parallel samples were taken as the results. The fatigue crack growth rate was measured with a compact tensile specimen. The surface area of the sample with a crack to be extended was polished to reduce the surface stress concentration. After the sample was clamped, the fatigue crack of 2 mm was prefabricated before the crack growth test. Sinusoidal wave loading was adopted. The stress ratio (R) was set at 0.1, and the frequency was 10 Hz. Each da/dN curve was measured with about three samples, and the da/dN data of compact tensile samples were measured with the crack opening displacement method (COD) automatically. The metallographic structure was observed by Axiocert 200 MAT microscope, and the microstructure, fatigue fracture morphology and second-phase particle energy spectrum analysis were observed by HITACHI-S4800 scanning electron microscope (SEM). In addition, about three samples were used for microstructural observation and mechanical properties at each location to confirm the repeatability and accuracy of the test. For the results with a large deviation, the number of samples would be expanded to find out the reasons for the error.

3 Results and discussion

3.1 Metallographic analysis

Figure 1 shows the three-dimensional metallography of the plate at different positions, and different grain structure characteristics are obtained. In Fig. 1, the grains at different positions both show typical fibrous microstructure, and they are severely elongated along the rolling direction, meanwhile, many second-phase particles are distributed in the microstructure. The grain size at D/4 (Fig. 1a) is larger than that at D/2 (Fig. 1b). And the difference of grain size is mainly caused by the inhomogeneous deformation during the rolling process and the subsequent heat treatment.

3.2 EBSD analysis

Figure 2 shows electron back-scattered diffraction (EBSD) maps and statistical results of grain size at different thickness positions of the plate.

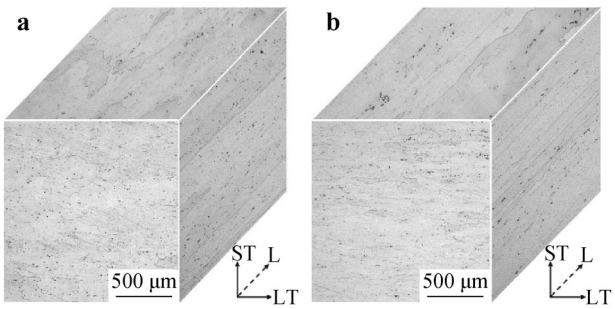

Fig. 1 Three-dimensional metallographies of 2624-T39 alloy at different positions: **a** D/4 position and **b** D/2 position

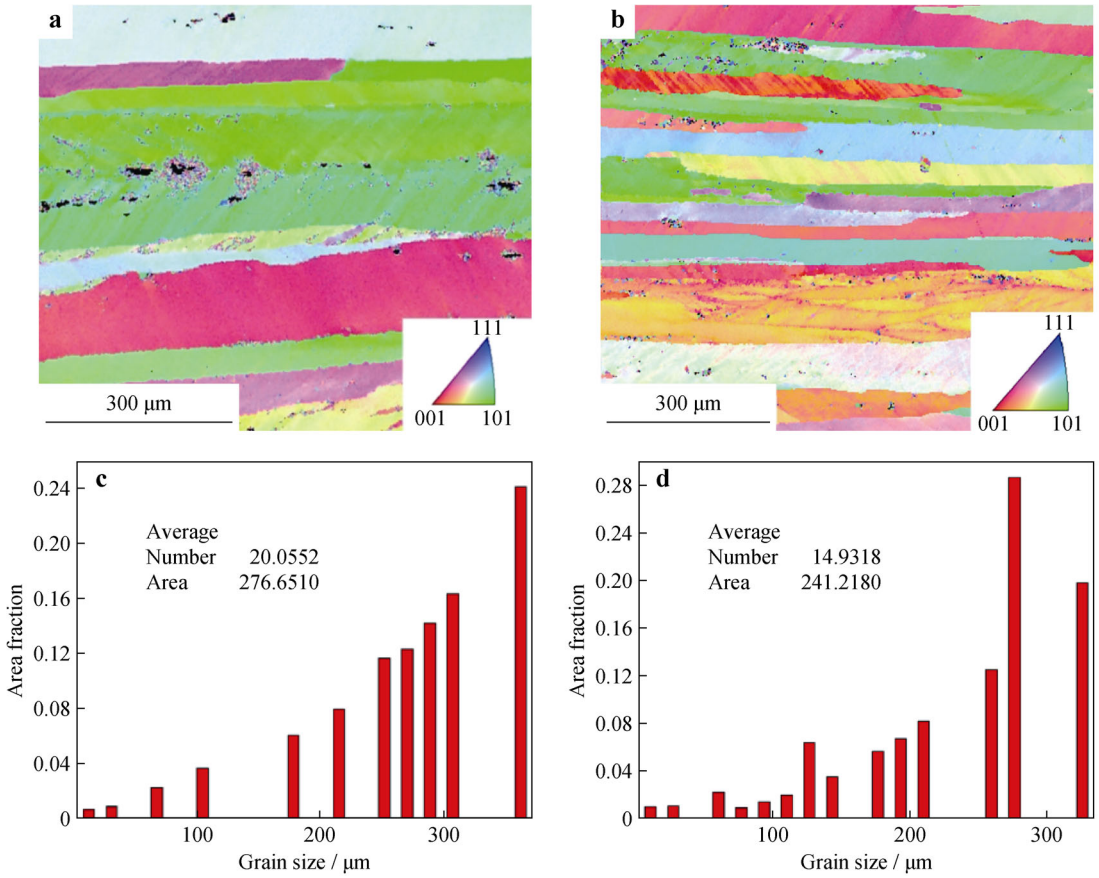

Fig. 2 EBSD maps of LS surface of alloy at **a** *D*/4 position and **b** *D*/2 position; statistical diagrams of grain size at **c** *D*/4 position and **d** *D*/2 position

According to Fig. 2a, b, the grains at *D*/4 and *D*/2 both show typical fibrous microstructure characteristics along the rolling direction. It is obvious that the grain size at *D*/4 is larger than that at *D*/2. The statistical results show that the grain size at *D*/4 is concentrated between 250 and 350 μm, and the average grain size is 276 μm. Meanwhile, the grain size at *D*/2 is concentrated between 200 and 300 μm, and the average grain size is 241 μm.

It can be seen from Fig. 2a, b that there are few grain boundaries in the rolling direction, while obvious grain boundaries can be seen in the width direction. So, we calculate the transverse particle width of multiple locations to obtain their average intercept. The average transverse length of grains at *D*/4 is 93.4 μm and that at *D*/2 is 65.3 μm. Therefore, it further indicates that the grain size at *D*/4 is larger than that at *D*/2.

3.3 SEM analysis

Figure 3 shows the SEM images of the plate in different thickness positions. It can be seen from Fig. 3a, c that a large number of undissolved coarse second-phase particles are distributed in microstructure, and some coarse phases are cracked. No obvious difference in amount, and distribution of the second phase is founded at *D*/4 and *D*/2 positions.

The undissolved phase mainly shows elliptic and rod-shaped. Table 1 shows the results of the energy spectrum analysis of the thick phase in Fig. 3. It can be seen from Table 1 that these undissolved thick second phases are mainly Al_2CuMg phase and Al_2Cu phase, and some second phases are Fe-rich phase and Mn containing phase. These undissolved phases are generally generated in the process of casting and homogenization, which have an adverse effect on the fatigue properties of materials. The main manifestations are as follows: with the increase of the size and amount of the undissolved second phase, the fatigue life of the alloy gradually decreases, and the fatigue crack growth rate gradually increases [20].

3.4 Conventional mechanical properties

Table 2 shows the tensile properties of 2624 aluminum alloys at *D*/2 and *D*/4 positions and the standard value of

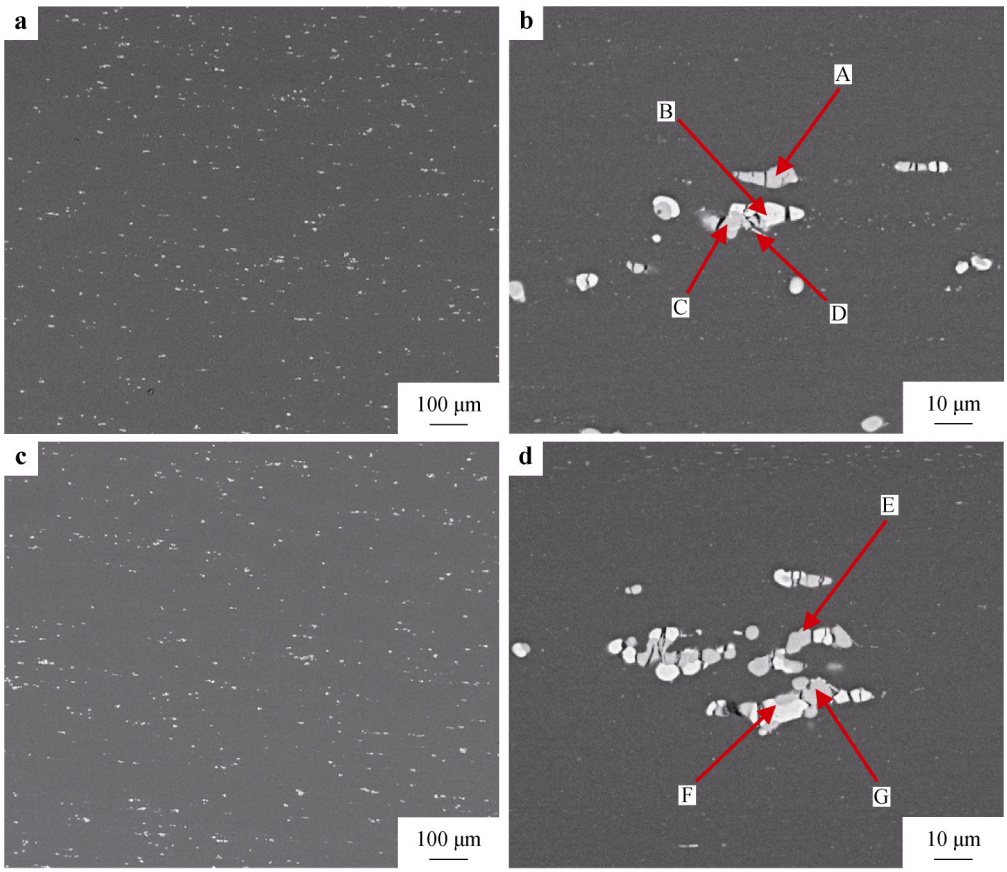

Fig. 3 SEM images of 2624-T39 alloy at **a, b** *D*/4 position and **c, d** *D*/2 position

Table 1 EDS analysis results of the phases in Fig. 3 (mol%)

Phases	Al	Cu	Mg	Fe	Mn
A	61.62	19.46	18.92	–	–
B	72.07	27.93	–	–	–
C	56.80	22.12	19.71	0.77	0.59
D	84.95	9.56	2.18	2.37	0.95
E	55.86	22.87	21.28	–	–
F	69.43	28.31	2.25	–	–
G	89.09	8.91	2.00	–	–

AMS 4473. It can be seen from Table 2 that the strength of the alloy varies in different orientation at the same position: the yield strength in the L (rolling) direction is significantly higher than that in the LT (transverse) direction, while the tensile strength in the L direction is slightly lower than that in the LT direction. The two positions show consistent regularity. In the L and LT directions, the tensile strength and yield strength at *D*/2 are slightly higher than that at *D*/4. Combined with the analysis of the metallographic structure photos in Fig. 1 and EBSD maps in Fig. 2, the alloy in both positions has a large amount of deformation structures, showing obvious anisotropy. The performance difference at different locations is mainly caused by grain size.

3.5 Fatigue crack growth performance

Figure 4a shows the relationship between crack length and cycle time. It can be observed that the growth rate of fatigue crack at *D*/4 is significantly lower than that at *D*/2. Figure 4b shows the curves of the fatigue crack growth rate at *D*/4 and *D*/2 positions. The test data were fitted according to the Paris formula, and the fatigue crack growth rate curve equation of Paris at two positions was obtained as

$$\left(\frac{\mathrm{d}a}{\mathrm{d}N}\right)_{D/2} = 1.12 \times 10^{-7}\Delta K^{2.91} \quad (1)$$

$$\left(\frac{\mathrm{d}a}{\mathrm{d}N}\right)_{D/4} = 3.05 \times 10^{-8}\Delta K^{3.36} \quad (2)$$

where $\mathrm{d}a/\mathrm{d}N$ is the fatigue crack growth rate and ΔK is the stress intensity factor.

There are three main stages in fatigue crack growth [21–23]: microcrack growth stage, macrocrack growth

Table 2 Mechanical properties of 2624-T39 aluminum alloy with different directions and positions

Alloys	Direction	Position	Tensile strength/MPa	Yield strength/MPa	Elongation/%
2624 (AMS4473)	L	–	469	427	10.0
	LT	–	490	400	8.0
2624-T39	L	*D*/2	529	478	9.5
	LT	*D*/2	534	451	8.0
	L	*D*/4	512	471	9.0
	LT	*D*/4	522	432	8.0

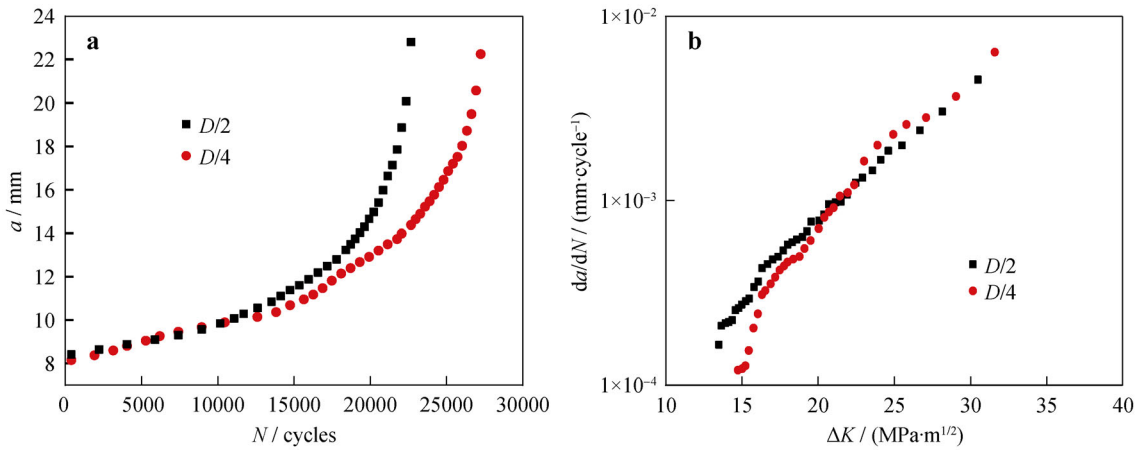

Fig. 4 Crack growth performance curve: **a** curve diagram of relationship between crack length (a) and cycle time (N); **b** crack growth rate curve of 2624 aluminum alloy

stage and instantaneous crack growth stage. By comparing the two curves in Fig. 4, it can be seen that the crack growth rate at the *D*/4 position is lower than that at the *D*/2 position, especially in the early stage of macrocrack growth, while the threshold value of crack growth at *D*/4 is significantly higher than that at *D*/2. Based on the analysis of the crack deflection model [15] and metallographic characteristics in Fig. 1, it can be concluded that the degree of crack deflection and crack closure at *D*/4 position with larger grain size is higher than that at *D*/2, which leads to lower fatigue crack growth rate.

In general, with the same ΔK, the effective driving force for the propagation of deflected crack is smaller than that for the propagation of straight crack [24–26]. On the other hand, the curved crack has a longer propagation path at the same distance than the straight crack, that is, the larger the grain size is, the longer the propagation path of the crack is at the same distance. [27, 28]. In addition, the crack closure is more obvious in coarse crystals due to the fracture mismatch, and the crack closure enhances the apparent driving force of the deflection crack growth [29]. Based on the above factors, coarse grains can obtain a lower fatigue crack growth rate.

3.6 Fatigue fracture analysis

Figure 5 shows the fracture morphology of fatigue crack growth at two locations of the alloy. It is found that the fracture morphology is mainly composed of three parts [30, 31]: the initial crack initiation zone, the steady-state crack growth zone and the transient fracture zone, among which the crack growth zone takes the largest proportion.

Figure 5a, b shows the region of low crack growth rate, where the cleavage steps, tearing edges and facets can be seen, and the fracture is serrated. By comparing the fractures at *D*/4 and *D*/2, it was found that the fracture at *D*/4 is relatively rough with a lot of bumpy small pits, while there are many small planes at *D*/2.

The morphology of the crack growth zone is shown in Fig. 5c, d. Obvious fatigue striations are found in the crack growth zone. Meanwhile, coarse second-phase particles are fractured during the process of fatigue crack growth, and some coarse second-phase particles fall off and form a large number of dimples on the fatigue striations. EDS analysis results of the second-phase composition are shown in Table 3, and the main compositions are Al_2CuMg phase and Al_2Cu phase.

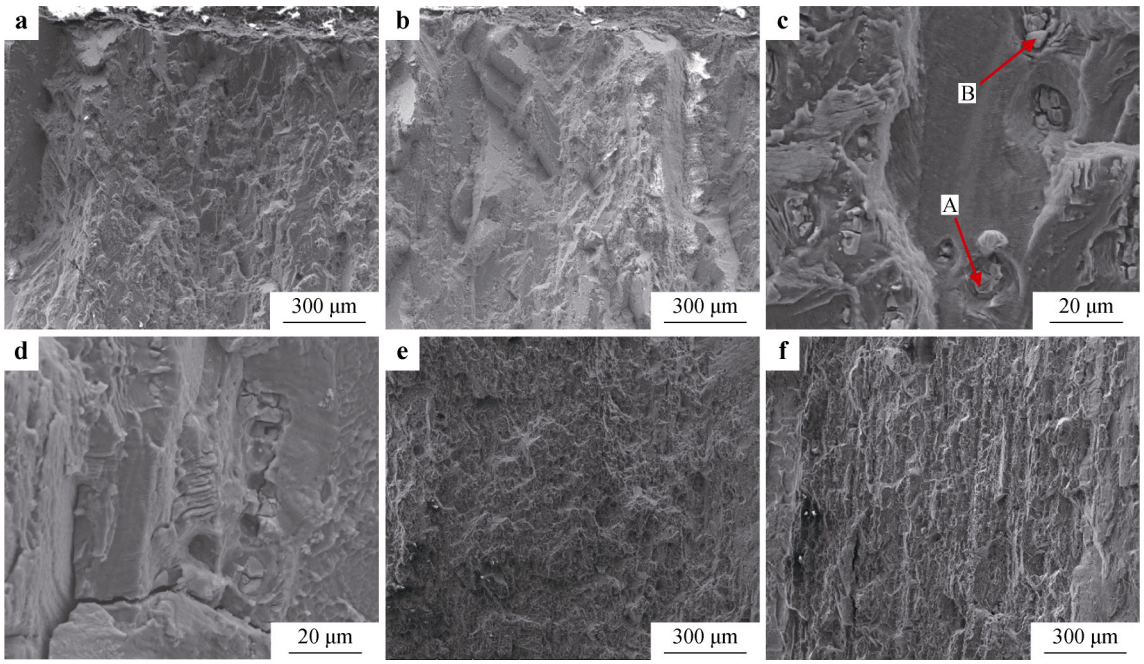

Fig. 5 Fatigue fracture SEM images of 2624-T39 aluminum alloy: initial crack initiation zones at **a** *D*/4 position and **b** *D*/2 position; steady-state crack growth zone at **c** *D*/4 position and **d** *D*/2 position; transient fracture zone at **e** *D*/4 position and **f** *D*/2 position

Table 3 EDS analysis results of the phases in Fig. 5 (mol%)

Phases	Al	Cu	Mg
A	52.12	26.21	21.67
B	71.53	28.47	–

Figure 5e, f shows the SEM images of instantaneous fault zones, in which a large number of dimples can be seen, and dimples are mixed with broken coarse second-phase particles. By comparing the morphology of the instantaneous fault zones at different thicknesses, it can be found that there are more small dimples at *D*/4.

4 Conclusion

Through the microstructure analysis and fatigue performance test of 2624-T39 thick plate alloy samples at *D*/4 and *D*/2 positions, the influences of microstructure characteristics of the alloy on the crack growth rate are as follows. The grain size of the 2624-T39 alloy was typically fibrous along the rolling direction, and the main second phase was Al_2CuMg. The average grain size at the *D*/4 position of the alloy was larger than that at *D*/2. The *D*/4 position with larger grain size showed lower fatigue crack growth rate, which may be attributed to the higher degree of crack deflection and crack closure. The fracture characteristics of the alloy at *D*/4 with low crack growth rate were as follows: the crack initiation area was relatively rough, the crack growth area had obvious fatigue striations, and the instantaneous fracture area had a large number of dimples with smaller size.

Acknowledgements This work was financially supported by the National Key R&D Program of China (No. 2016YFB0300800).

References

[1] Eto T, Nakai M. New process-microstructure method for affordable 2024 series aerospace aluminum alloys. Mater Sci Forum. 2007;539–543:3643.
[2] Dursun T, Soutis C. Recent developments in advanced aircraft aluminium alloys. Mater Des. 2014;56:862.
[3] Heinz A, Haszler A, Keidel C, Moldenhauer S, Benedictus R, Miller WS. Recent development in aluminium alloys for aerospace applications. Mater Sci Eng A. 2000;280(1):102.
[4] Starke EA Jr, Williams JC. Progress in structural materials for aerospace systems. Acta Mater. 2003;51(19):5775.
[5] Srivatsan TS, Kolar D, Magnusen P. The cyclic fatigue and final fracture behavior of aluminum alloy 2524. Mater Des. 2002; 23(2):129.
[6] Ge RS, Zhang YA, Li ZH, Wang F, Zhu BH, Xiong BQ. Fatigue crack growth rate and microstructures of 2E12 and 2524 alloy. Chin J Rare Met. 2011;35(4):600.
[7] Tiamiyu AA, Basu R, Odeshi AG, Szpunar JA. Plastic deformation in relation to microstructure and texture evolution in AA 2017-T451 and AA 2624-T351 aluminum alloys under dynamic impact loading. Mater Sci Eng. 2015;636:379.
[8] Thompson AW, Backofen WA. The effect of grain size on fatigue. Acta Metall. 1971;19(7):597.

[9] Zurek AK, James MR, Morris WL. The effect of grain size on fatigue growth of short cracks. Metall Trans A (Phys Metall Mater Sci). 1983;14(8):1697.
[10] Zhang G, Gang L, Ding X, Sun J, Tong Z, Shao Y, Chen K. A fatigue model of high strength Al alloys containing second phase particles of various sizes. Rare Met Mater Eng. 2004;33(1):35.
[11] Saga J, Hayashi M, Nishio Y. Effect of grain size on fatigue crack propagation in aluminium. J Soc Mater Sci Jpn. 1977;26: 1202.
[12] Lindigkeit J, Terlinde G, Gysler A, Lütjering G. The effect of grain size on the fatigue crack propagation behavior of age-hardened alloys in inert and corrosive environment. Acta Metall. 1979;27(11):1717.
[13] Carter RD, Lee EW, Starke EA, Beevers CJ. The effect of microstructure and environment on fatigue crack closure of 7475 aluminum alloy. Metall Mater Trans A. 1984;15(3):555.
[14] Shou WB, Yi DQ, Liu HQ, Tang C, Shen FH, Wang B. Effect of grain size on the fatigue crack growth behavior of 2524-T3 aluminum alloy. Arch Civ Mech Eng. 2016;16(3):304.
[15] Yin DY, Liu HQ, Chen YQ, Yi DQ, Wang B, Shen FH, Fu S, Tang C, Pan SP. Effect of grain size on fatigue-crack growth in 2524 aluminium alloy. Int J Fatigue. 2016;84:9.
[16] Valiev RZ, Islamgaliev RK, Alexandrov IV. Bulk nanostructured materials from severe plastic deformation. Prog Mater Sci. 2000;45(2):103.
[17] Plekhov O, Paggi M, Naimark O, Carpinteri A. A dimensional analysis interpretation to grain size and loading frequency dependencies of the Paris and Wohler curves. Int J Fatigue. 2011;33(3):477.
[18] Yang HX, Li JS, Guo T, Wang WY, Kou HC, Wang J. Evolution of microstructure and hardness in a dual-phase Al0.5CoCrFeNi high-entropy alloy with different grain sizes. Rare Met. 2020; 39(2):156.
[19] Händel M, Nickel D, Lampke T. Effect of different grain sizes and textures on the corrosion behaviour of aluminum alloy AA6082. Mater Werkst. 2011;42(7):606.
[20] Chen YQ, Pan SP, Zhou MZ, Yi DQ, Xu DZ, Xu YF. Effects of inclusions, grain boundaries and grain orientations on the fatigue crack initiation and propagation behavior of 2524-T3 Al alloy. Mater Sci Eng A. 2013;580:150.
[21] Wang J, Fang C, Hao H, Wang SH, Yang SJ, Dai SL, Zhang XG. Effects of trace Zr on the microstructure and properties of 2E12 alloy. Rare Met. 2009;28(5):511.
[22] Dominguez J, Zapatero J, Pascual J. Effect of load histories on scatter of fatigue crack growth in aluminum alloy 2024-T351. Eng Fract Mech. 1997;56(1):65.
[23] Golestaneh AF, Ali A, Bayat M. Analytical and numerical investigation of fatigue crack growth in aluminum alloy. Key Eng Mater. 2011;462–463(4):1050.
[24] Suresh S. Fatigue crack deflection and fracture surface contact: micromechanical models. Metall Trans A (Phys Metall Mater Sci). 1985;16(1):249.
[25] Cavaliere P. Fatigue properties and crack behavior of ultra-fine and nanocrystalline pure metals. Int J Fatigue. 2009;31(10): 1476.
[26] Padilla HA, Boyce BL. A review of fatigue behavior in nanocrystalline metals. Exp Mech. 2010;50(1):5.
[27] Pokluda J. Dislocation-based model of plasticity and roughness-induced crack closure. Int J Fatigue. 2013;46(1):35.
[28] Turnbull A, Rios ERDL. The effect of grain size on fatigue crack growth in an aluminium magnesium alloy. Fatigue Fract Eng Mater Struct. 2010;18(11):1355.
[29] Tan L, Zhang XY, Xia T, Huang GJ, Liu Q. Fracture morphology and crack mechanism in pure polycrystalline magnesium under tension–compression fatigue testing. Rare Met. 2020;39(2):162.
[30] Haigen J, Zhimin Y, Feng J, Xue L. EBSD analysis of fatigue crack growth of 2124 aluminum alloy for aviation. Rare Met Mater Eng. 2014;43(6):1332.
[31] Yamada R, Itoh G, Kurumada A, Nakai M. Further study on the effect of environment on fatigue crack growth behavior of 2000 and 7000 series aluminum alloys. Mater Sci Forum. 2016;879: 2153.